



Long-Term Impact of Historical Mining on Water Quality at Mount Lyell, Western Tasmania, Australia

Sibele C. Nascimento¹  · David R. Cooke^{1,2} · Ashley T. Townsend³ · Garry Davidson² · Anita Parbhakar-Fox^{2,4} · Matthew J. Cracknell^{1,2} · Clare B. Miller^{1,2}

Received: 6 October 2022 / Accepted: 7 July 2023 / Published online: 19 July 2023
© The Author(s) 2023

Abstract

During the twentieth century, inadequate management of mine waste at the Mount Lyell Copper Mine affected the ecology of the Queen–King Rivers and Macquarie Harbour, western Tasmania, Australia. Over the past two decades, the water quality of the river system has been measured semi-annually to investigate the long-term hydrochemical and environmental impacts caused by these historical mine practices and the waste associated with the Mount Lyell mine to the Queen–King Rivers. At sample sites below the confluence of Haulage Creek, the water pH was below pH 3.5, remaining below pH 5 across all sites to Macquarie Harbour. Local baseline rivers ranged from pH 4.0 to 8.4. Elemental concentrations of dissolved metals in water samples downstream of Haulage Creek were above the Australian and New Zealand Environment and Conservation Council (ANZECC) water quality guidelines. Copper, Fe, and Zn were not attenuated along the length of the river, with concentrations remaining elevated to the King River Delta. Mineralogical analyses demonstrated secondary minerals in sediments at Haulage Creek and pyrite concentrated at the King River Delta. Static tests on mining-affected sediments indicated risk of AMD and metal(loid) leaching in the river system. Since 2016, after flooding of the Prince Lyell mine, dissolved metal levels in the Queen–King Rivers have decreased; however, concentrations remain above guidelines. Almost three decades after legacy mine waste disposal ended, it still poses a long-term risk to the downstream environment, implying that without effective management of these historical mine wastes, the Queen–King Rivers will continue to be severely impacted.

✉ Sibele C. Nascimento
s.nascimento@uq.edu.au

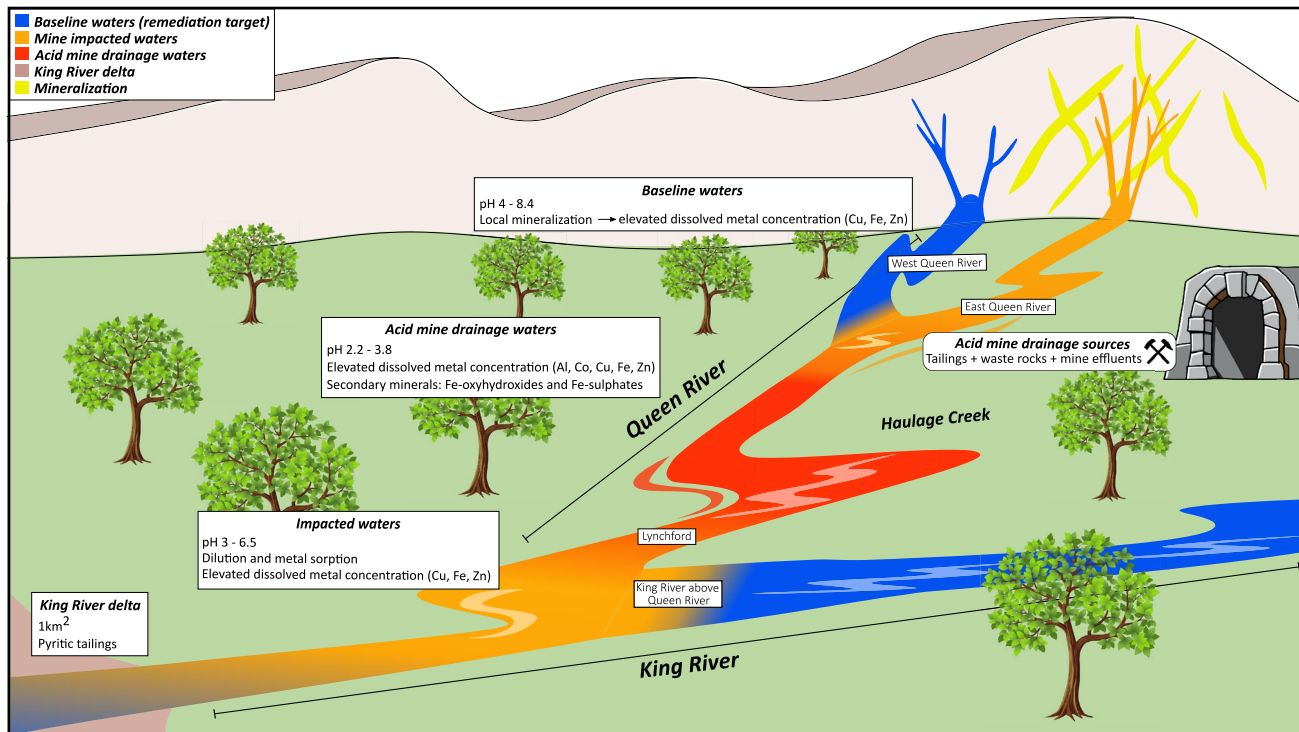
¹ Transforming the Mining Value Chain, University of Tasmania, TAS, Private Bag 79, Hobart 7001, Australia

² Centre for Ore Deposit and Earth Sciences, University of Tasmania, TAS, Private Bag 79, Hobart 7001, Australia

³ Central Science Laboratory, University of Tasmania, TAS, Private Bag 74, Hobart 7001, Australia

⁴ W. H. Bryan Research Centre, Sustainable Minerals Institute, University of Queensland, 40 Isles Road, Indooroopilly, QLD 4068, Australia

Graphical Abstract



Keywords Acid mine drainage · Tailings · Metal(lloid)s · Water quality · Waste disposal · Pollution · Rehabilitation

Introduction

Acid mine drainage (AMD) generates pollution from geochemical sources as well as anthropogenic activities that continues to be an important environmental problem, with mitigation of their impacts remaining a challenge globally (Sheoran and Sheoran 2006). The United Nations has emphasised the significance of this environmental challenge by acknowledging it as the second greatest global issue after human-induced climate change (Qian and Li 2019). One of the most significant AMD cases in Australia is associated with the Mount Lyell copper mine in Queenstown, western Tasmania. From 1893 to 2014, Cu, Ag, and Au were extracted and processed at Mount Lyell. Between 1893 and 1994, mineral processing was initially achieved via pyrite smelting (until 1969) and then via flotation (initiated in 1916) to preconcentrate copper (McQuade et al. 1995). By-products of these operations included: atmospheric release of sulfur dioxide (SO_2) fumes and large volumes of AMD, smelter slag, waste rock, and tailings (McQuade et al. 1995), which were disposed of into Haulage Creek (Fig. 1) leading to contamination in the Queen–King River system. During operations, the disposal of mine wastes from Mount Lyell into the

receiving environment was considered the highest continuous mine-sediment discharge into any river system in Australia (Olive and Reiger 1986).

While tailings discharge stopped in 1994, the mine wastes still remain in the overbanks and bottom of the Queen and King Rivers (Locher 1997). It is estimated that 10–87 million tonnes (Mt) of mining-impacted sediments have accumulated at the King River Delta and in the surrounds of Macquarie Harbour (Augustinus et al. 2010; Locher 1997). Taylor et al. (1996) investigated how the acid and metals release by these waste deposits have affected the river system, but the short-term period of the survey (6 days) prevented a detailed long-term assessment of this complex, dynamic, and evolving hydrogeochemical system and its chemical processes. Additionally, other authors performed extensive research in the area prior to (EGI 1991, 1993; Mt Lyell 1990) and after tailings dumping ceased in 1994 (Davies et al. 1996; Klessa et al. 1997; Locher 1997). Although providing basis for the characteristics of the Queen–King Rivers, these studies do not give information on the current conditions of the river. Investigation into the rivers water quality and sediment chemistry would also benefit from methods currently available, such as paste pH and NAG pH tests.

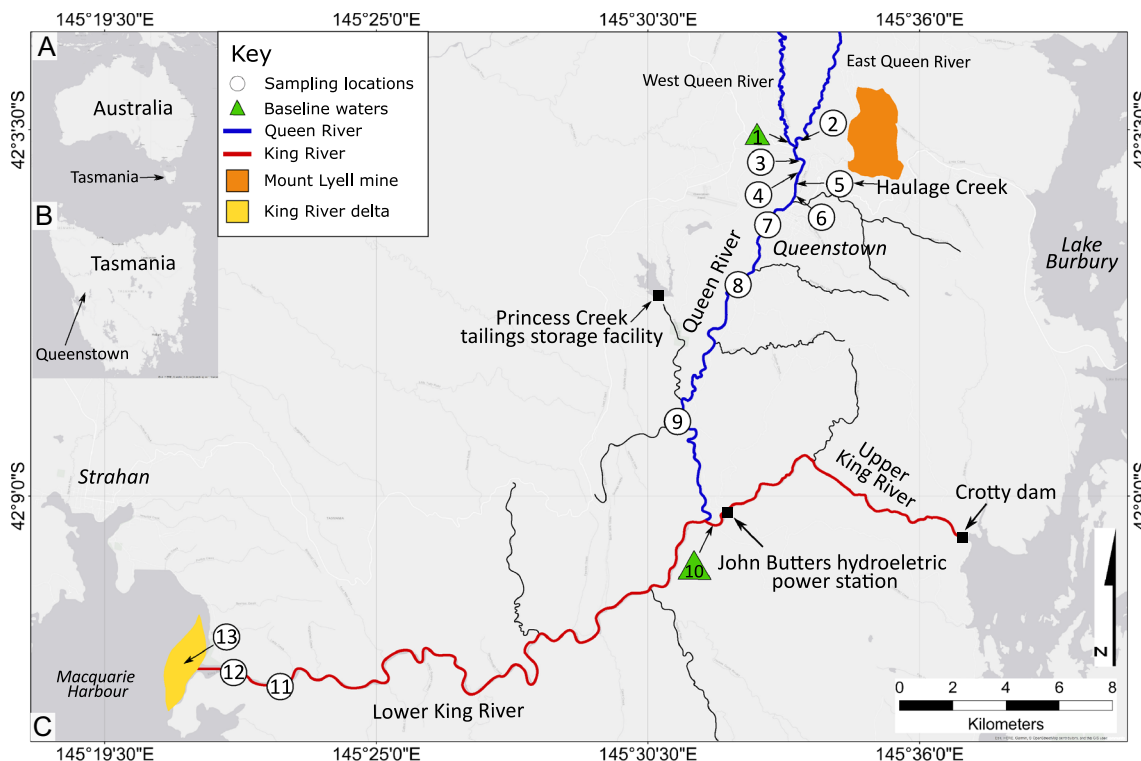


Fig. 1 A Map of Australia; B map of Tasmania showing Queenstown where the Mount Lyell mine is located; C Mount Lyell mine situated north of Queenstown. The Queen River system is displayed in blue, and the King River system is displayed in red. The King River delta is located at the confluence with Macquarie Harbour. The Princess Creek tailings dam built by Copper Mines of Tasmania (CMT) and the power station that dammed the King River are also shown.

For the past 2 decades (2001–2021), researchers from the University of Tasmania (UTAS) have monitored the water chemistry of the Queen–King River system by sampling 13 locations annually. Based on the observations of this long-term monitoring project, this study aims to: (i) assess long-term trends in water quality [i.e. pH, electrical conductivity (EC), and metal(lloid)s]; (ii) characterise the geochemistry and mineralogy in the river sediments; (iii) determine the variation of physico-chemical parameters along the Queen–King River system; and (iv) assess the potential of tailings to generate AMD using static tests. The present study provides an up-to-date study on the condition of the Queen–King River system as well as longitudinal data to evaluate the long-term environmental effects of mine waste disposal on the Queen–King River system. These findings aim to provide useful long timeline data that will help identify appropriate remediation strategies and inform future environmental management of mine sites in western Tasmania.

Sampling locations: (1) West Queen River; (2) East Queen River; (3) Mine Entrance; (4) Queen above Haulage Creek; (5) Haulage Creek (HC); (6) Queen below Haulage Creek; (7) Austin St Park; (8) Golf Club; (9) Lynchford; (10) King River above Queen River; (11) Bank D; (12) Bank A; (13) King River delta. Triangles represent baseline waters (sites 1 and 10)

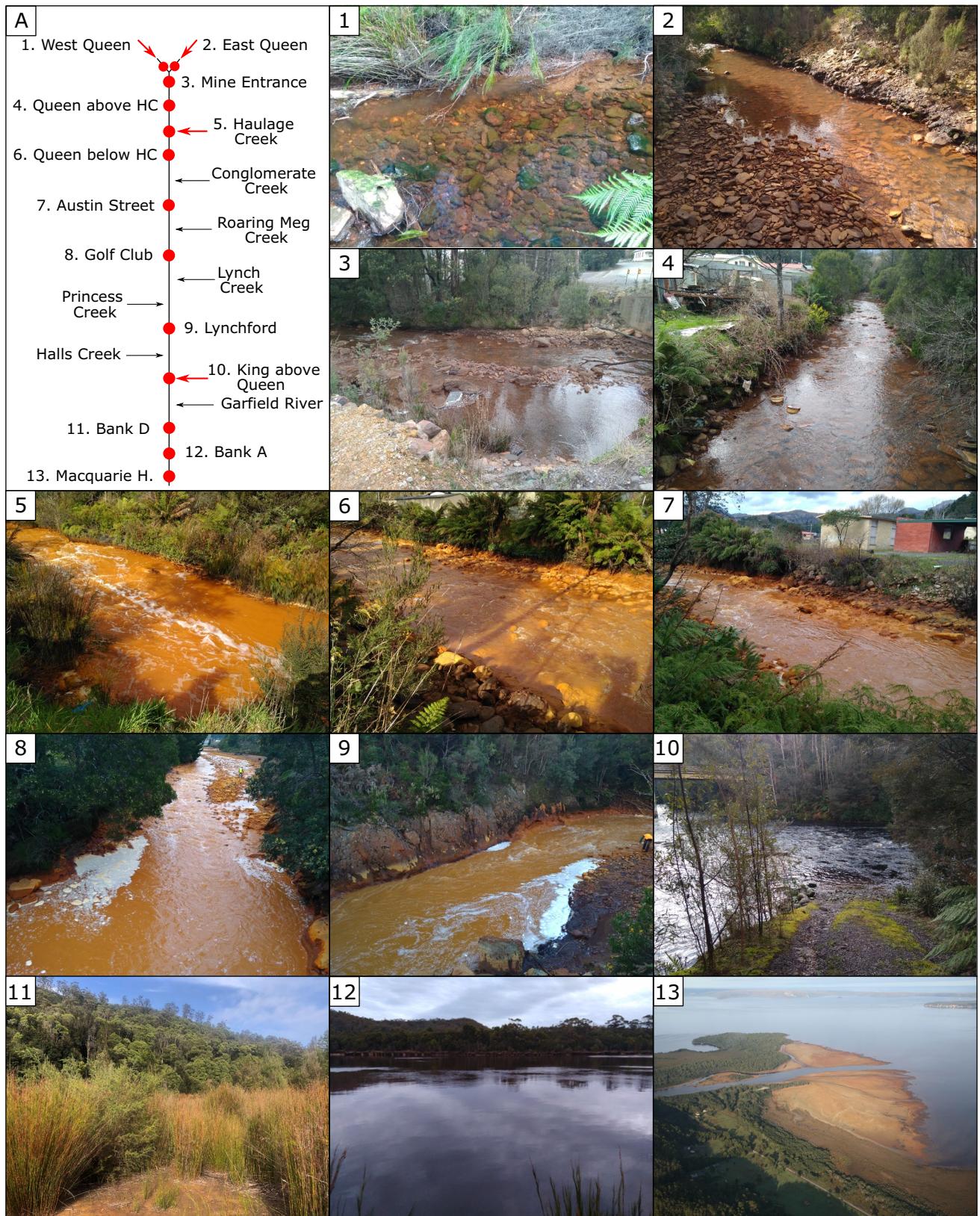
Study Location, Mining History and Geology

Mining operations at Mount Lyell were initiated in 1893 and ceased in 2014. The Mount Lyell Mining & Railway Company (MLMRC) operated from 1893 to 1994. In 1995, the mine was taken over by Gold Mines of Australia, which was later renamed Copper Mines of Tasmania (CMT). Since then, operations carried out by CMT have been highly regulated and to date, operated to best practice as required by their licenses. For more information about Mount Lyell mining operations, geology, waste characteristics, regulations, and climate of the region, refer to the Supplementary File.

Materials and Methods

Field Sampling and Sample Preparation

The Queen–King River system and the King River Delta were sampled at 13 sites semi-annually from 2001 to 2021



◀Fig. 2 A Schematic of inputs and sampling locations of the Queen–King River system with numbers representing sites displayed in Fig. 1. Sites shown in order from above the mine site (1–West Queen) to 13–Macquarie Harbour. West Queen (1) and King River above Queen (10) sites represent baseline waters. Site 10 dilutes AMD. Clear signs of AMD are observed at Haulage Creek (5) and downstream (6–9). *Juncus pallidus*, a species usually observed at impacted mine sites across Tasmania, is detected at Bank D (11). Tailings deposited on the King River Delta in Macquarie Harbour (13) is shown

($n=16$), typically in September (i.e. spring). Note that data are scarce in the early years (i.e. from 2001 to 2006) and only few parameters [i.e. pH and dissolved metal(lloid)s] were measured at sites 4, 5, and 6. From 2007, water quality measurements were taken yearly (excluding 2010) at all sites (except when conditions were adverse). Water samples were routinely collected using grab samples, both up and downstream of the confluence with the mining discharge (Figs. 1 and 2). Two unimpacted sites (sites 1 and 10) were sampled to establish baseline water quality for the region. At each location pH, Eh, EC, and metal(lloid) concentrations were measured. All data are provided in supplemental Table S-2. In 2018, sediment grab samples from the rivers were also collected at the same locations for mineralogical and geochemical analysis except at Bank D (site 11).

Water quality was measured in the field using calibrated portable devices. Values of pH and temperature were obtained using an Eutech PC 450 portable device that was calibrated before analysis to pH 4 and pH 7. Electrical conductivity was measured using a WP-84 Conductivity-TDS-Sal-Temp instrument and calibrated before measurements against certified EC standards (1413 and 12,880 $\mu\text{S}/\text{cm}$). A Milwaukee MW 500 portable device was used to measure Eh. Flow rate was assessed using a Global Flow Probe (FP101–FP201). After each measurement, water samples were collected and filtered through 0.45 μm PES filters to differentiate between dissolved and particulate components (although some researchers suggest 0.2 μm enables a better discrimination, even 0.1 μm for Al; Baird and Bridgewater 2017). Samples were then placed into 50 mL HDPE bottles and were acidified with 1 mL of 1% HNO_3 to a pH of < 2 . Samples were kept refrigerated prior to later metal(lloid)s analysis at the University of Tasmania (UTAS) laboratories.

Sediment samples were collected and, on return to the UTAS laboratories, were dried in a furnace at 40 °C for several days. Oversized material (> 4 mm) was crushed, with samples milled in a chrome steel ring mill for 3 min (to < 75 μm) to obtain a homogenous material for geochemical analysis and static tests.

Geochemical and Mineralogical Analysis

Dissolved metal(lloid)s in collected water samples were measured using sector field inductively coupled plasma mass spectrometry (SF-ICP-MS). Over the duration of this study, two instrument models were employed, “Element 1” and “Element 2” (Thermo Fisher, Bremen, Germany). Both instruments possessed multiple resolution settings enabling interference-free determination of low mass isotopes relevant to this study (Townsend 1999, 2000). Indium was added to all samples as an internal standard, with quantitation via external calibration. Instrument performance and calibration accuracy were verified each analytical sequence through the routine analysis of external certified reference waters. For example, the average accuracy of aluminium (Al), cadmium (Cd), cobalt (Co), copper (Cu), iron (Fe), nickel (Ni), lead (Pb), and zinc (Zn) measured in NIST 1640a Trace Elements in Water over 10 years was $100 \pm 4\%$. Given the high matrix load and variable acidity/salinity of collected waters, samples were typically diluted by a factor of 50 prior to analysis.

Bulk element composition (trace: As, Cd, Cu, Ni, Pb, Zn) of the sediment samples was assessed using a portable X-ray fluorescence (p-XRF) device (Vanta handheld XRF analyser) in soil mode. This handheld device was calibrated at the start of each analysis session. In-house rock standard TASBAS (basalt) and international standard reference materials GXR4/541 (Cu mill head powder) and RTS-3 (sulfide ore mill tailings) were assessed at the beginning and end of each analysis period. Analysis for total N, C, H, and S was determined using a Thermo Finnigan EA 1112 Series Flash Elemental Analyser. Between 7 and 10 mg of sample were weighed into tin capsules using a Sartorius SE2 ultramicrobalance with an accuracy of 0.1 μg . Combustion of the pressed tin cups was achieved in ultra-high purity oxygen at 1000 °C using tungsten oxide on alumina as an oxidising agent, followed by reduced copper wires as a reducing agent. Results were generated following calibration against a certified sulphanilamide standard.

The water quality guidelines applied in this study (pH, EC, dissolved metals) are defined by ANZECC (supplementary Table S-3; ANZECC 2000). Note that trigger values (concentrations that, if exceeded, would indicate a potential environmental problem) for Al, Cu, and Zn are for aquatic freshwater (90% species protection). Cobalt and Fe have insufficient data to derive reliable trigger values for freshwater (ANZECC 2000), so irrigation water elements trigger values were used.

Mineralogical analysis of river sediments ($n=12$) was performed by powder X-ray diffraction (XRD) using a benchtop Bruker D2 Phaser X-ray diffractometer (Bruker AXS GmbH, Karlsruhe, Germany). Prior to analysis, each sample was spiked with $\approx 10\%$ by total sample mass of pure corundum powder and milled with an agate pestle and

mortar to $<10\text{ }\mu\text{m}$. The samples were analysed for 30 min between 4° and 90° 20 with 0.02° step size and counting 0.5 s per step. Mineral phases were identified using a Bruker DIFFRAC.EVA software package and the PDF-2 (2012 release) powder diffraction file database. Mineral abundances were quantified using TOPAS Rietveld analysis software (version 4.2).

The mineral morphology of river sediments samples ($n=4$) was examined by scanning electron microscopy (SEM). A Hitachi SU-70 field-emission scanning electron microscope (FE-SEM) fitted with a five-segment solid state BSE detector and an Oxford Instruments Aztec EDS system equipped with an x-max 80 SDD EDS detector was used with the operating volume set at 1.5 kV for imaging. Polished grain mounts (3 cm diameter) were carbon-coated prior to analysis. Oxford Aztec software was used to assist data processing.

Static Tests

Paste pH and advanced net acid generating (NAG) tests (Weber et al. 2006) were undertaken using a calibrated Eutech PC 450 portable device on pulverised samples to evaluate the acid-producing nature of collected river sediments. For paste pH, 20 mL of deionised water was added to 10 g of samples at a solid to water ratio of 1:2 (w/w) and stirred. The slurry was allowed to stand overnight and subsequently the pH was measured directly in the slurry, following the methodology outlined by Smart et al. (2002). The NAG test involved the addition of 250 mL of H_2O_2 to 2.5 g of pulverized sample as per Smart et al. (2002). Total sulfur was analysed prior to NAG testing to estimate the H_2O_2 concentration required. Samples with $<0.3\%$ S had 15% H_2O_2 added, while samples with $>0.3\%$ S were treated with 30% H_2O_2 . H_2O_2 was added in three stages to ensure complete sulfide oxidation:

1. 100 mL of H_2O_2 was added to samples and left for 2 h;
2. A further 100 mL of H_2O_2 was added and left for another 2 h;
3. Finally, 50 mL of H_2O_2 was added to the mixture and was left to react overnight.

The following day, the samples were gently heated to accelerate the oxidation of the remaining sulfides. When cool, the NAG pH was measured, and the leachates were collected and filtered with $0.45\text{ }\mu\text{m}$ PES filters into 50 mL HDPE bottles prior to SF-ICP-MS analysis.

Mass Loads Estimation of Metals

The mass loads (ML, $\text{kg}\cdot\text{day}^{-1}$) of metals in the Queen–King River system were calculated by:

$$\text{ML} = \text{Q} * \text{C} \quad (1)$$

where ML is the calculated mass load ($\text{mg}\cdot\text{time unit}^{-1}$), Q is the flow rate ($\text{litres}\cdot\text{time unit}^{-1}$) in the Queen–King River system and C is the concentration ($\text{mg}\cdot\text{L}^{-1}$) of metals. Because the flow rate was measured in $\text{m}\cdot\text{s}^{-1}$, conversion into volume was required:

$$Q(\text{L}\cdot\text{s}^{-1}) = 1000 * \text{W} * \text{D} * \text{F} \quad (2)$$

where W is the width of the river (m), D is the depth of the river (m), and F is the measured flow rate ($\text{m}\cdot\text{s}^{-1}$). Substituting Eq. (2) in (1) and converting $\text{mg}\cdot\text{s}^{-1}$ into $\text{kg}\cdot\text{day}^{-1}$, the estimated daily metal mass load in a sample site of the Queen–King River system is:

$$\text{ML}(\text{kg}\cdot\text{day}^{-1}) = 86.4 * \text{W} * \text{D} * \text{F} * \text{C} \quad (3)$$

Statistical Analysis

Box plots were built for descriptive statistics of the Queen–King River system water quality, using ioGAS-64 software version 6.3. Correlation matrix was built using the Spearman method to obtain the association between metal(lloid)s measured in sediments by pXRF. The correlation matrix was generated with the same software.

Results

The following sections present the main results obtained in this study considering samples collected over the past two decades from the Queen–King River system. Results are presented for stream sediments, providing geochemistry and mineralogy of the river sediments, followed by water quality measurements [pH, EC, Eh, and dissolved metal(lloid)s], and finally characterisation of the AMD potential of the sediments and waters.

Stream Sediments

Geochemical Characteristics

Elemental concentrations of metal(lloid)s of the Queen and King Rivers sediments measured by pXRF are displayed in Fig. 3 and supplemental Table S-4. Concentrations are compared to ANZECC interim sediment quality guidelines (ISQG), which contain two alert concentrations (i.e.

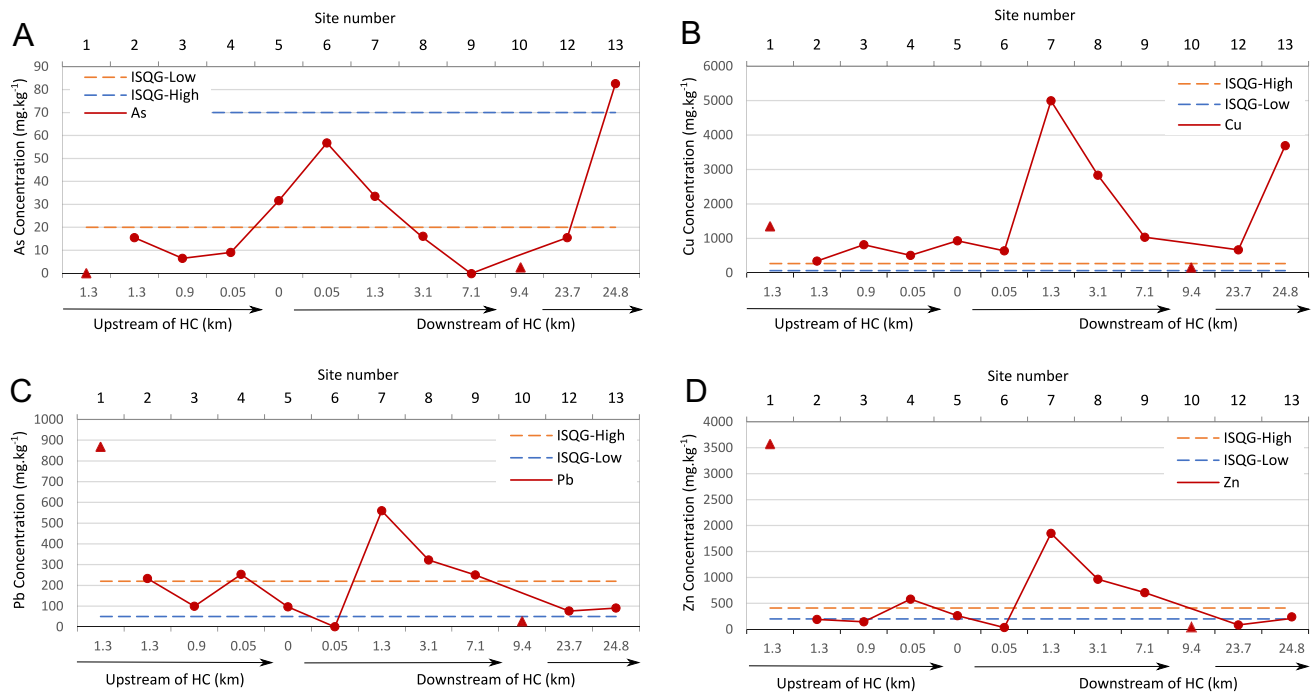


Fig. 3 Metal(loid)s content (mg·kg⁻¹; measured by p-XRF) in stream sediments at the Queen-King River system. Triangles are baseline waters (sites 1 and 10). ANZECC (2000) ISQG-Low and ISQG-High values indicated by dash lines for comparison. Site numbers are

shown and represent the locations addressed on Fig. 1. Distance is from each location to Haulage Creek (HC), where tailings and effluent discharge occurred. Site 10 is located in the upper King River, not downstream of Haulage Creek

ISQG-low and ISQG-high, supplemental Table S-5). The King River above the Queen River sample (site 10, uncontaminated) contained concentrations of As (3 mg·kg⁻¹), Cu (60 mg·kg⁻¹), Pb (25 mg·kg⁻¹), and Zn (40 mg·kg⁻¹) below the ISQG-low values (ANZECC 2000). Baseline concentrations in the West Queen River sample (site 1) exhibited metal concentrations above the ISQG-High guideline (Cu = 1350 mg·kg⁻¹; Pb = 870 mg·kg⁻¹, Zn = 3570 mg·kg⁻¹). Arsenic was below the ISQG-High value throughout the river, except at the delta (site 13), where its concentration was 80 mg·kg⁻¹. Copper concentrations were above the ISQG-High values in the entire extent of the Queen and King River (besides site 10), with contents ranging from 345 mg·kg⁻¹ at the East Queen River (site 2) to 5000 mg·kg⁻¹ at Austin St. Park (site 7). Lead concentrations fluctuated in sediment samples, ranging from concentrations below detection limits downstream of Haulage Creek (site 6) to 870 mg·kg⁻¹ at the West Queen River (site 1), exceeding ISQG-High values at sites 1, 4, 7, 8, and 9. Similarly, Zn concentrations varied spatially with sites 1, 4, 7, 8, and 9 exceeding ISQG-High values. Zinc values ranged from 35 mg·kg⁻¹ downstream of Haulage Creek (site 6) to 3570 mg·kg⁻¹ at the West Queen River (site 1). Lead and Zn showed similar trends of spatial distribution.

Concentrations of As, Cu, Pb, and Zn were plotted against sulfur (S) and Fe (Fig. 4) to examine their spatial distribution

in the Queen–King River system and potential mineral hosts. The greatest S concentration is observed in the delta samples (site 13), where high amounts of pyrite is present (Table 2). As and Cu are also high concentrations at this location. Iron appears enriched at Haulage Creek and downstream (sites 5 and 6), whereas these sites are depleted in Cu, Pb, and Zn when compared to sites 7 and 8. Arsenic typically increases with increasing S and Fe and is highly correlated with both metals (Fig. 4, Table 1). Lead and Zn concentrations are linked, displaying similar trends with regards to S and Fe.

Mineralogical Characterisation

Field observations indicate clear waters with tannins and uncoated pebbles in the West Queen River and the King River above Queen River (Fig. 2, sites 1 and 10). Haulage Creek and locations downstream contain Fe-coated pebbles and sand to fine sand particles with clear signs of AMD as observed from Fe precipitates [“yellow boy”, Fig. 2(5–9)]. The tailings-rich sediment deposited in Macquarie Harbour are sand-sized with visible organic matter (e.g. leaves and twigs), slag, and grains of pyrite.

Semi-quantitative XRD analysis of mineralogy from all the sampled sites is presented in Table 2. The King and Queen Rivers are dominated by sediments consisting of (in decreasing order of significance) quartz, muscovite,

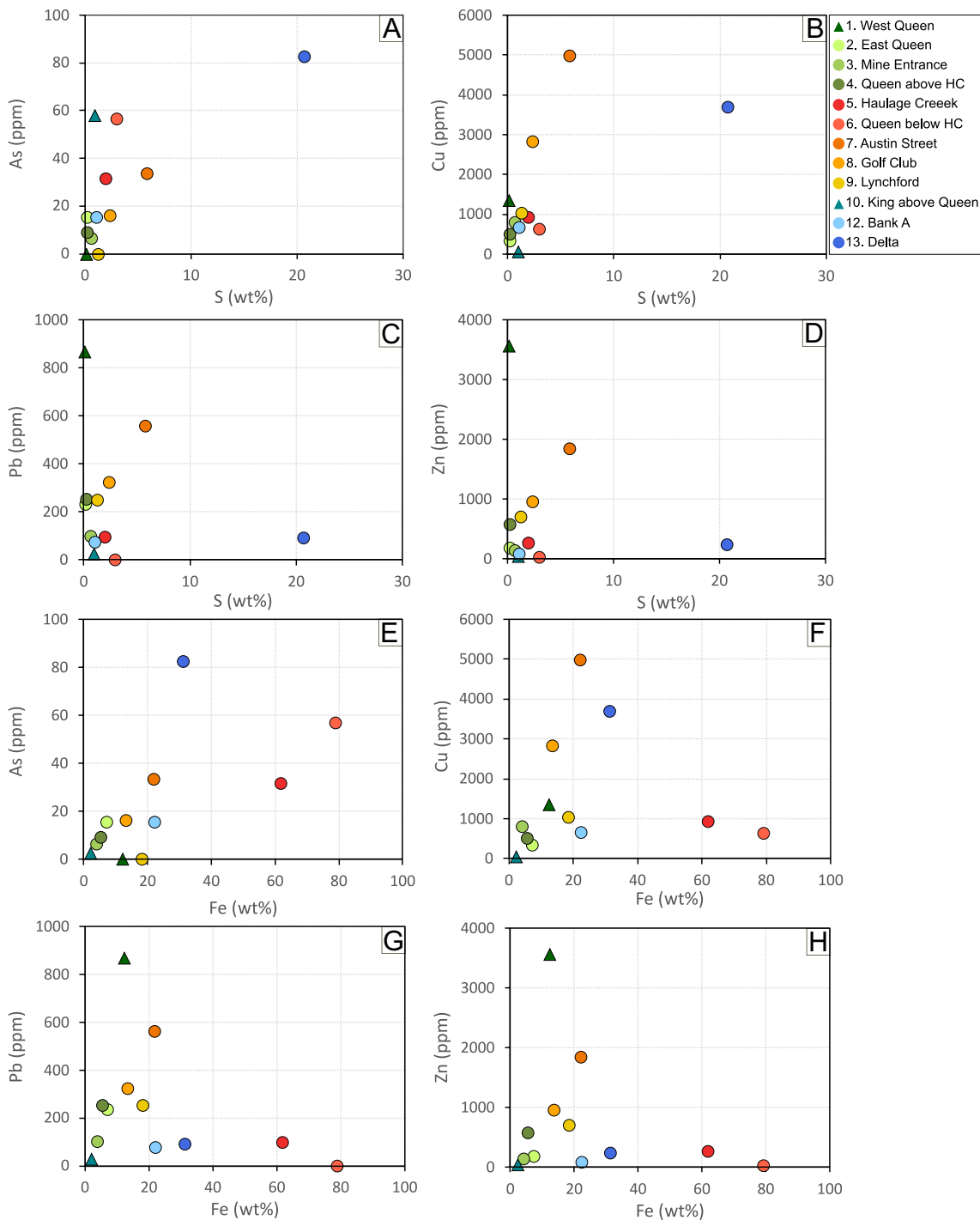


Fig. 4 Concentrations of As, Cu, Pb and Zn (mg.kg⁻¹; measured by XRF) against S (wt%) and Fe (mg.kg⁻¹) for the Queen–King River sediments

chlorite, and ferrihydrite. Pyrite is the major sulfide phase at sites 7 (5 wt%) and 13 (18 wt%). Secondary minerals such as goethite and hematite were identified, especially at and downstream of Haulage Creek (sites 5 and 6), where goethite appears as the primary mineral phase (Table 2). Trace amounts of chalcopyrite were observed at sites 7, 8,

and 13, corresponding to the increased Cu concentrations observed in the bulk sediment (Fig. 3). No carbonates were observed within these sediments.

Grain morphology, particle size, sphericity, and mineral associations of sulfide minerals (pyrite and chalcopyrite) within the sediments were examined with the SEM.

Table 1 Correlation Matrix of metal(lloid)s measured in sediments in 2018 by pXRF

	As	Cu	Fe	Pb	S	Zn
As	1					
Cu	0.66	1				
Fe	0.88	0.42	1			
Pb	0.3	0.51	0.064	1		
S	0.88	0.57	0.71	-0.22	1	
Zn	0.24	0.69	0.042	0.92	0.073	1

Iron-bearing minerals were found to rim finer pyrite grains (50 µm diameter, Fig. 5A) at Haulage Creek. Framboidal pyrite (20 µm diameter, Fig. 5B) was observed at Haulage Creek as well as pyrite encapsulated by quartz (Fig. 5C). At depths greater than 0 to 10 cm below the delta surface, coarser grains of moderately angular, liberated pyrite (i.e. not associated with other minerals) were encountered (150 µm diameter, Fig. 5D). Finer pyrite grains were also observed in association with chlorite. Fine grains of chalcopyrite (30 µm diameter) encapsulated by weathered chlorite (Fig. 5E) and iron oxide coating (Fig. 5F) on mineral grains were observed in shallow sediments.

Given the limitations of XRD for the identification of mixed grains of poorly crystalline or nanocrystalline phases, high amounts of unknown/amorphous material were reported (Table 2). The mineralogy of the fine-grained sediment at Haulage Creek and the King River Delta (sites 5 and 13) were further investigated by SEM–EDS (Figs. 5 and 6 and Supplementary Fig. S-1). Mineral chemistry shows Fe ranging from 50 to 72 wt%, O from 27 to 42 wt%, and S up to 6 wt%. This chemical composition and morphology suggests

that these grains are Fe-oxyhydroxysulphate, normally precipitated at AMD sites (e.g. schwertmannite, jarosite, and ferrihydrite) that latter transform to more crystalline phases (i.e. hematite and goethite; Durocher and Schindler 2011; España 2007; Guo and Barnard 2013; Williamson et al. 2006). However, the mineralogy of these authigenic mixed materials were inconclusive as SEM also poses certain limitations in accurately distinguishing Fe-oxyhydroxysulphate, including alteration through heat or dehydration of samples, lack of H quantification in EDS spectra, small differences in Fe–O ratios, and interaction with neighbouring particles.

Water Chemistry

Physiochemical Parameters

At the West Queen River (site 1), the median pH is 6.0 (supplementary Table S-2) with a low value measured in 2021 (i.e. pH=4). At the King River above Queen (site 10), the pH ranges from 5.7 to 8.4. These baseline waters displayed the lowest EC with median 0.09 and 0.07 mS/cm values, respectively (Fig. 7G). Site 1 had the lowest Eh median of the region, calculated as 193 mV (Fig. 7H). Site 10 showed an Eh median of 287 mV. The effect of the tailings discharge is apparent at East Queen River (site 2), the first site post outfall, where the pH drops markedly below 4. Increases in pH is represented by outliers at sites 2 and 3 (i.e. 2019 and 2017, respectively), still showing acidic conditions. Higher oxidizing conditions are noted at site 2, with an Eh median of 500 mV.

At Haulage Creek (site 5), low pH values were consistently recorded over the past decades (2.2–3.8; Fig. 7F). The median EC was the highest of the studied area (4.9

Table 2 Bulk mineralogy (measured by XRD in wt%) of stream sediments of the King and Queen Rivers and delta (BDL=below detection limits of <0.2%)

Mineral	Formula	1	2	3	4	5	6	7	8	9	10	12	13
Quartz	SiO ₂	37.6	58.0	58.5	59.5	22.6	8.1	39.0	43.2	52.2	59.0	40.0	29.0
Muscovite	KAl ₂ (AlSi ₃ O ₁₀)(OH) ₂	6.6	12.0	15.0	10.2	4.1	1.1	8.0	10.3	5.9	9.3	8.0	6.7
Chlorite	Mg ₅ Al(AlSi ₃ O ₁₀)(OH) ₈	3.7	8.6	9.0	6.1	5.6	4.5	6.6	8.0	7.0	3.7	8.3	9.4
Ferrihydrite	Fe ³⁺ ₁₀ O ₁₄ (OH) ₂	1.7	3.1	3.0	2.5	1.4	0.5	2.3	2.7	2.7	2.3	3.0	2.4
Albite	NaAlSi ₃ O ₈	3.7	0.8	6.0	2.0	BDL	BDL	2.0	0.8	BDL	3.5	0.3	BDL
Goethite	α-Fe ³⁺ O(OH)	BDL	BDL	BDL	BDL	22.0	21.0	0.3	BDL	0.3	BDL	0.2	BDL
Magnetite	Fe ²⁺ Fe ³⁺ ₂ O ₄	0.2	0.5	0.4	0.6	1.0	1.6	1.1	0.5	0.7	0.2	0.9	0.9
Hematite	Fe ₂ O ₃	BDL	1.2	BDL	0.2	0.2	BDL	0.8	0.2	0.3	0.9	0.0	1.7
Jarosite	KFe ³⁺ ₃ (SO ₄) ₂ (OH) ₆	0.2	BDL	0.2									
Pyrite	FeS ₂	BDL	BDL	0.4	BDL	0.2	0.7	5.0	1.7	BDL	BDL	0.3	17.7
Chalcopyrite	CuFeS ₂	BDL	BDL	BDL	BDL	BDL	BDL	0.5	0.3	BDL	BDL	BDL	0.2
Pyrophyllite	Al ₂ Si ₄ O ₁₀ (OH) ₂	BDL	2.0	BDL	1.4	BDL							
Unknown		46.3	14.2	8.0	17.5	43.1	62.4	34.7	32.5	30.7	21.3	39.2	32.0

Location numbers are shown and represent the sites addressed on Fig. 1

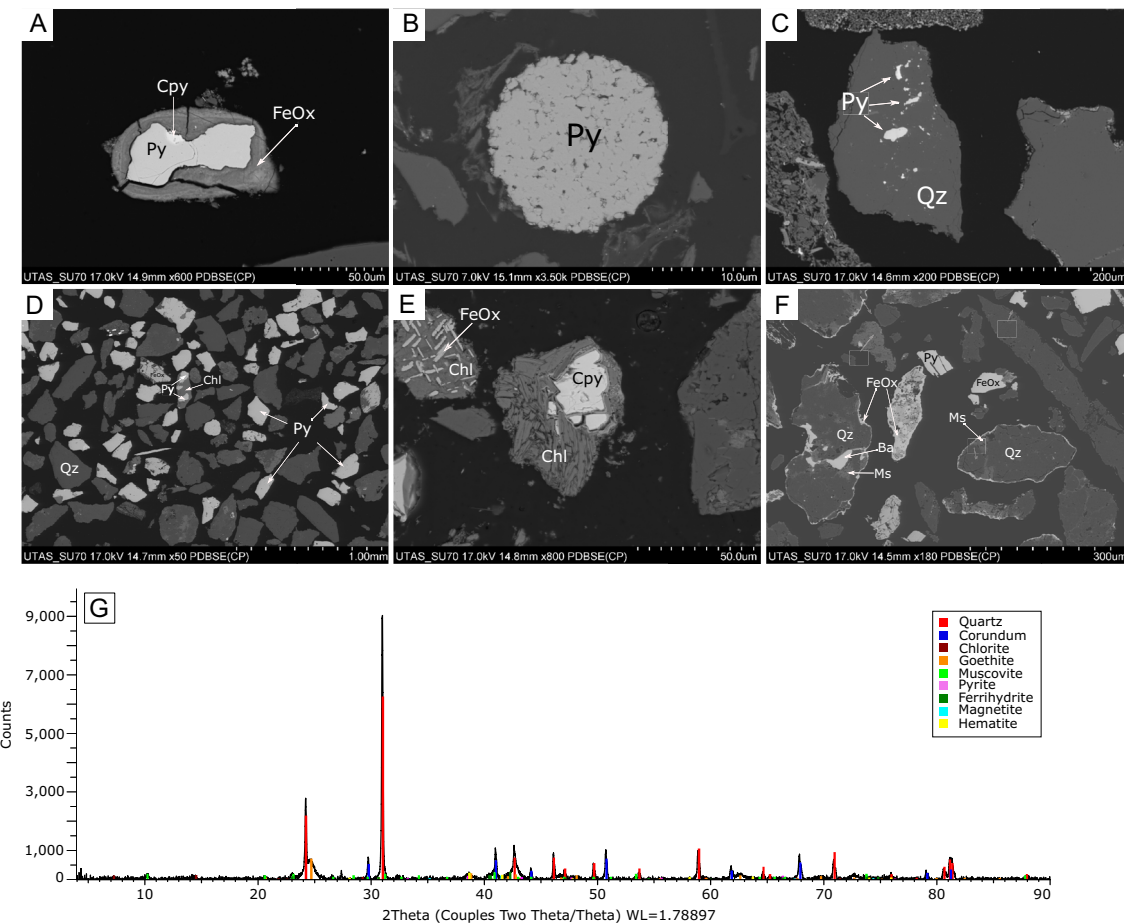


Fig. 5 A–C SEM images of sediments from Haulage Creek; D–F SEM images of sediments from the delta (Chl, chlorite; Cpy, chalcopyrite; FeOx, Fe-oxyhydroxysulphate; Ms, muscovite; Py, pyrite; Qz, quartz) G XRD patterns of sediments from Haulage Creek

mS/cm), ranging from 0.9 to 7.5 mS/cm (Fig. 7G). Below Haulage Creek (site 6) to Lynchford (site 9), there was a slightly decrease in acidity; however, the pH remained below 4. Additionally, from site 5 to site 9, higher Eh values were recorded, with medians from 468 to 493 mV.

At site 11, the pH was found to increase compared to upstream locations. Although the pH varied in the past decade below the junction of the Queen with the King River, a low median pH was observed ($\text{pH} < 4.5$), indicating that the effect of the tailings discharge remains, and the King River displays acid characteristics. High salinity from sea water contributes to Macquarie Harbour samples displaying the greatest EC variation (Fig. 7G), with a minimum of 0.02 mS/cm and maximum of 11.1 mS/cm from 2008 to 2021. A decrease in Eh was noticed, with median values ranging from 334 mV at site 11 to 260 mV at site 13.

Dissolved Metals in Stream Waters

The dissolved metals in Fig. 7A–E (i.e. Al, Co, Cu, Fe, Zn) were selected for water quality assessment, based

on their higher concentration in the river, their environmental concerns and potential health hazards, and their economic value (e.g. Co, Cu). Distribution of data indicates similar trends for all dissolved metals analysed. Their lowest concentrations were noted at baseline sites 1 and 10 (Fig. 7). Metal concentrations increase between site 2 and 4, reaching peak levels at Haulage Creek, where Al, Co, Cu, Fe, and Zn contents were in the ranges of $70\text{--}180 \text{ mg}\cdot\text{L}^{-1}$, $1\text{--}3 \text{ mg}\cdot\text{L}^{-1}$, $11\text{--}70 \text{ mg}\cdot\text{L}^{-1}$, $195\text{--}1200 \text{ mg}\cdot\text{L}^{-1}$, and $2\text{--}13 \text{ mg}\cdot\text{L}^{-1}$, respectively. Water samples collected in 2016 displayed the lowest concentrations for Al ($98 \text{ mg}\cdot\text{L}^{-1}$), and Fe ($220 \text{ mg}\cdot\text{L}^{-1}$) when the highest pH (3.0) was documented in Haulage Creek. Metal concentrations remain high downstream of Haulage Creek to Lynchford. Cobalt is observed to be above Australian guidelines (ANZECC 2000) from Haulage Creek (site 5) to Lynrd (site 9), while Al, Cu, Fe, and Zn exceed guidelines at all sampling locations.

The calculated mass load of Co and Cu entering the Queen and King Rivers are given in Supplemental Table S-2. The percentage of Co and Cu in the river system

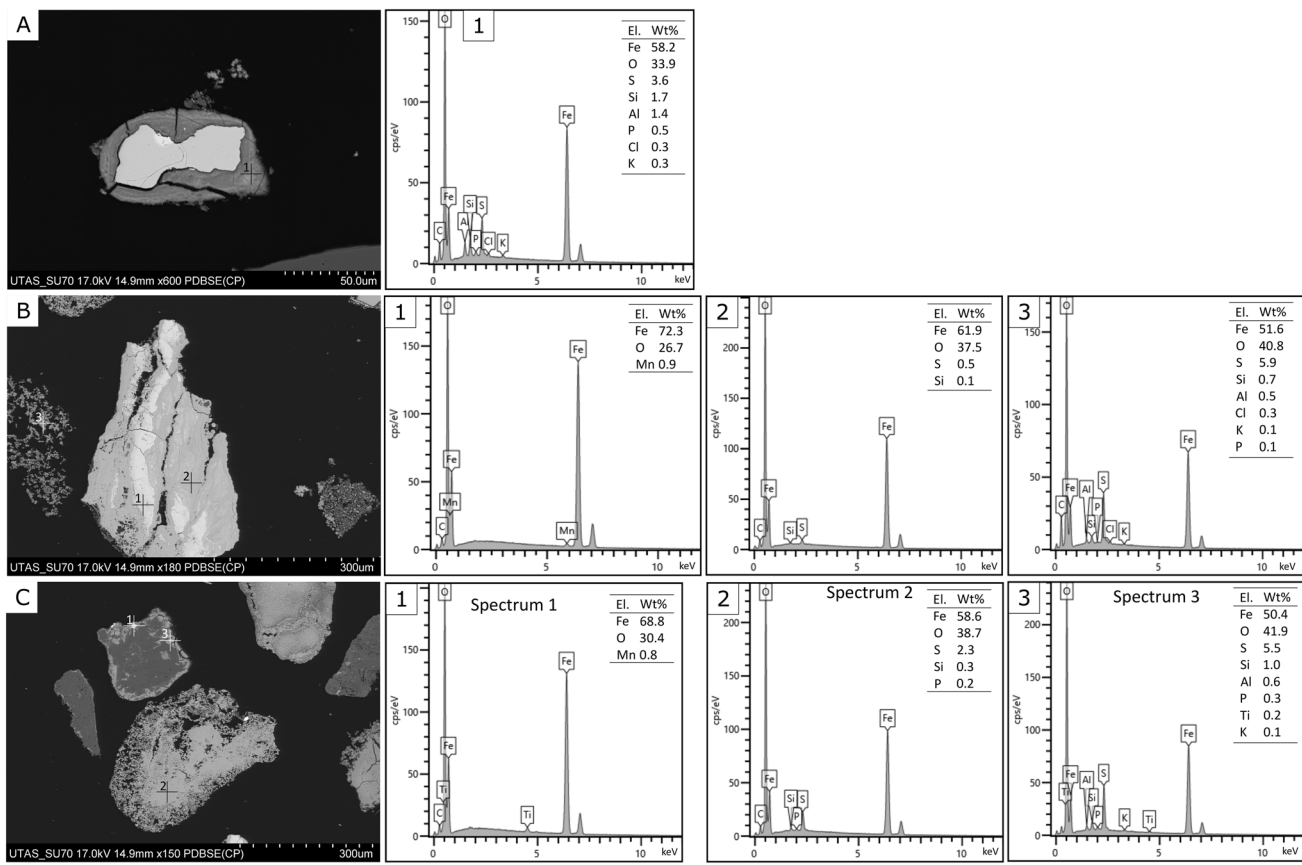


Fig. 6 SEM images and EDS spectra of sediments from Haulage creek showing elements (El.) and respective composition (Wt%). Crosshairs demonstrate location of EDS analysis, note that symbol is larger than beam diameter

being contributed from Haulage Creek ranges from Co 13.5 wt% to 55.8 wt% and Cu 12.6 wt% to 56.1 wt%. From 2012 until 2019, Co mass load in Haulage Creek ranged from ≈ 115 to $848 \text{ kg}\cdot\text{day}^{-1}$ while Cu ranged from 712 to $12,520 \text{ kg}\cdot\text{day}^{-1}$. Haulage Creek contributed 65 t of Co and 492 t of Cu in 2019. Although Haulage Creek contributes the highest mass load entering the Queen River, 2020 and 2021 flow rate data are not available in this catchment and for this, mass loads relating to the Austin St. site 7 (catchment closer to Haulage Creek with available data) were used for an up-to-date trend (Fig. 7I). Mass load reached its highest level of Co at $325 \text{ kg}\cdot\text{day}^{-1}$ and Cu at $6971 \text{ kg}\cdot\text{day}^{-1}$ in 2013 but has since declined, reaching values of Co $55 \text{ kg}\cdot\text{day}^{-1}$ and Cu $688 \text{ kg}\cdot\text{day}^{-1}$ in 2021.

Characterisation of AMD Potential

Static testing on sediment samples collected during 2018 was undertaken to predict AMD lag time, and longevity of acid formation as recommended by Price (1997) and Weber et al. (2006) (Table 3). According to their classification,

baseline samples (sites 1 and 10) are non-acid forming (Fig. 8A), whilst most of the river sediments (sites 2, 3, 4, 7, 8, and 13) were of medium risk and likely to form acid rapidly. Sediments collected at sites 5, 6 and 9 were of high risk with immediate acid generation likely to occur.

The sum of dissolved base metals Cd, Co, Cu, Ni, Pb, and Zn measured in the Queen–King River system were plotted against pH (Fig. 8B) as per Plumlee et al. (1999), as well as As (Fig. 8C) and Al (Fig. 8D). Dissolved metals in NAG leachates against NAG pH (Table 3) were also plotted. Accordingly, Haulage Creek can be classified as highly acidic (pH 2.2–3.0), with high metal(lloid) contents. As expected, baseline sites can be considered near-neutral (site 1, pH 4.0–7.1 and site 10, pH 5.7–7.8) with low dissolved metal(lloid) concentrations. Waters upstream of Haulage Creek (sites 2, 3, and 4) are mostly acid (median pH 3.5, 4.2, 4.5 respectively) with low metal(lloid) contents. Downstream of Haulage Creek (sites 6, 7, 8, and 9), samples displayed a median pH of 2.9–3.0 and high metal concentrations. The remaining streams are typically classified as pH acid with low metal(lloid) dissolution.

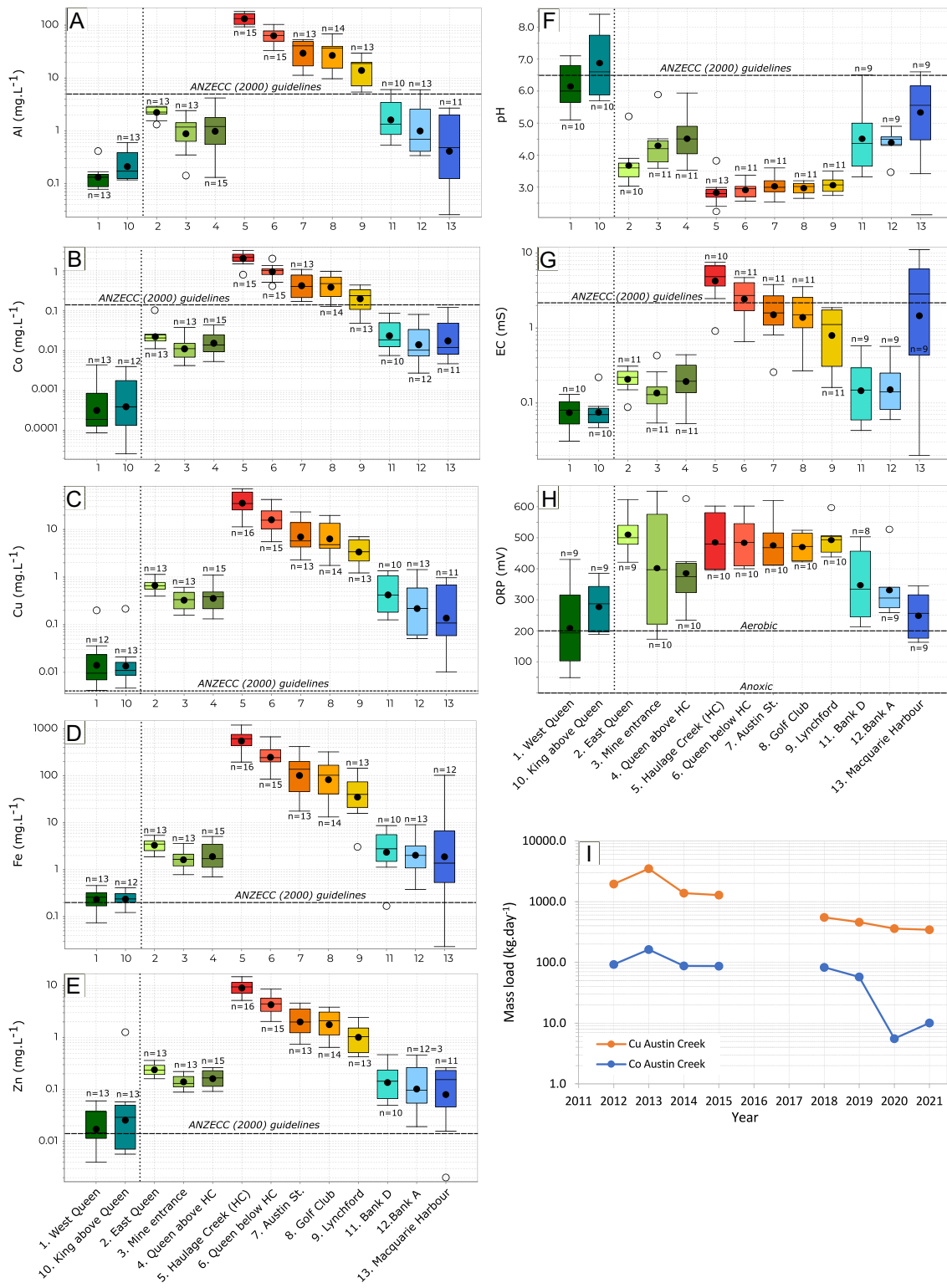


Fig. 7 Boxplots showing average dissolved metal(lloid)s ($\text{mg}\cdot\text{L}^{-1}$; measured by ICP-MS), pH, EC (mS/cm) and Eh (mV) in water catchments of the Queen and King Rivers from 2001 to 2021. The box shows the 25th percentile and the 75th percentile, and the whiskers represent the smallest and largest values. The lines inside the box are

the median and the black circle is the mean of the population. Locations are displayed in the graphic with baseline waters (sites 1 and 10) on the left-hand side. ANZECC guideline values are represented by the dashed lines for comparison. **A** Al; **B** Co; **C** Cu; **D** Fe; **E** Zn; **F** pH; **G** EC; **H** Eh; **I** mass load of Cu and Co

Table 3 Paste and NAG pH values obtained from sediments in Queen–King Rivers

Sample ID	Paste pH	NAG pH	Metals in NAG leachates (mg.L^{-1})					
			Cd	Co	Cu	Ni	Pb	Zn
1. West Queen	6.8	5.2	0.00	0.00	0.02	0.00	0.00	0.01
2. East Queen	5.0	3.8	0.00	0.02	0.7	0.03	0.05	9.9
3. Mine Entrance	5.3	2.6	0.00	0.2	9.1	0.04	0.03	0.7
4. Queen above HC	4.9	3.3	0.00	0.06	2.5	0.03	0.03	0.4
5. Haulage Creek	2.4	2.6	0.00	0.2	5.4	0.07	0.07	1.4
6. Queen below HC	2.7	2.4	0.00	0.2	0.2	0.03	0.08	0.6
7. Austin Street	4.6	2.6	0.01	1.1	51.2	0.1	0.04	15.7
8. Golf Club	5.1	2.7	0.00	0.7	30.8	0.09	0.05	7.9
9. Lynchford	3.0	2.6	0.00	0.2	6.2	0.04	0.05	4.1
10. King above Queen	7.4	5.5	0.00	0.00	0.0	0.00	0.00	0.01
12. Bank A	4.0	2.7	0.00	0.3	5.3	0.06	0.07	0.8
13. Delta	4.6	2.2	0.00	1.9	27.5	0.3	0.00	1.2

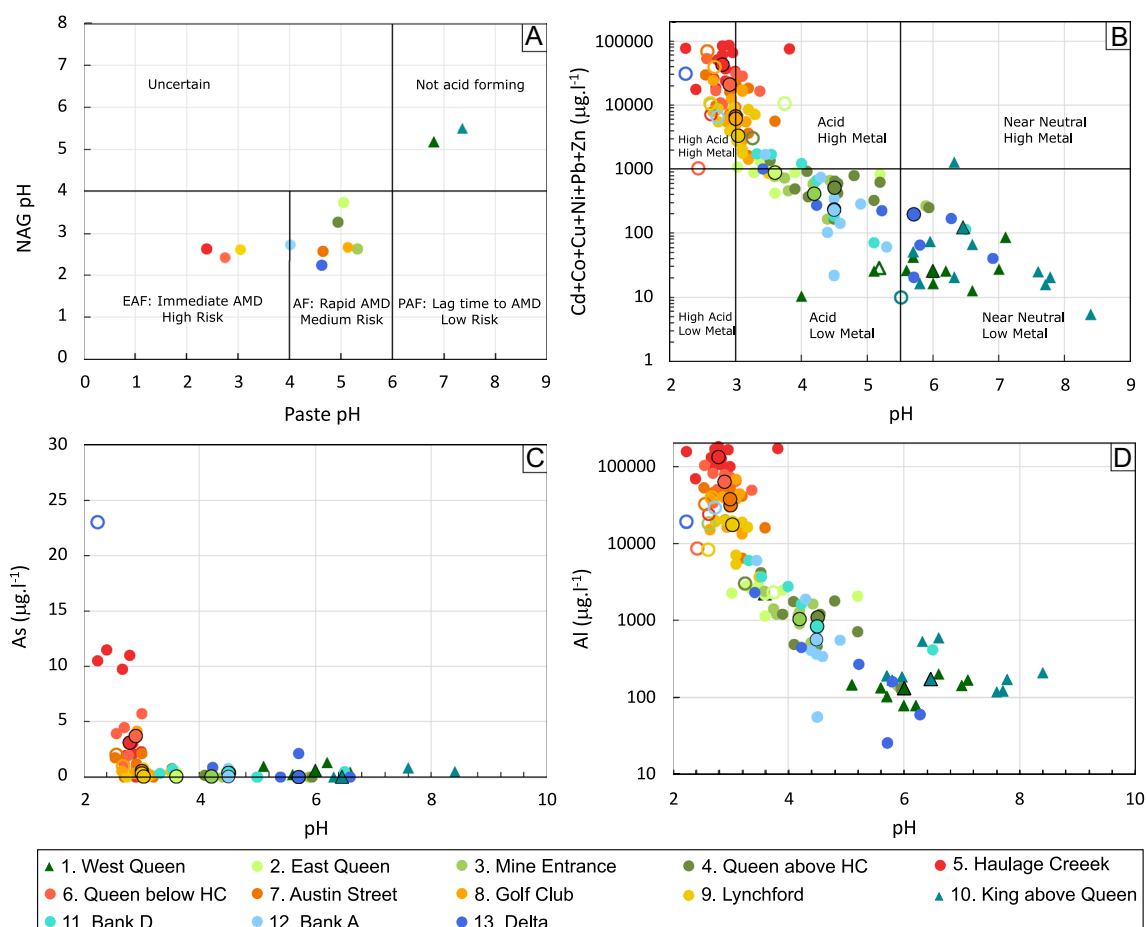


Fig. 8 **A** Classification of acid forming potential and lag-time to acid formation at the Queen and King Rivers sediment samples based on NAG pH versus paste pH. **B** Ficklin diagram classifying waters and leachates from sediments collected across the Queen–King River system based on the sum of dissolved base metal(lloid)s Cd, Co, Cu, Ni, Pb and Zn against pH, as proposed by Plumlee et al. (1999). Plot

of pH against **C** As and **D** Al. Filled shapes represent water chemistry collected over the past two decades. Void shapes represent leachate measurements from NAG tests on sediments collected in 2018. Larger black lined shapes represent the median of the field-based dataset. Triangles are baseline waters (EAF extremely acid forming, AF acid forming, PAF potentially acid forming)

Ficklin plots (Fig. 8B) characterise most of the NAG leachates as highly acidic with high dissolved metals (sites 3, 5, 6, 7, 8, 9, 12, 13). Sites 2 and 4 were acid with high metal concentrations, while baseline waters were classified as acid with low metal release (site 1), and low acid with low metal contents (site 10).

Discussion

Sources of AMD to the Queen–King River System

Discharge of mine waste and AMD from Haulage Creek into the Queen–King River system resulted in changes in water quality and morphology of the river that persist to the present day (i.e. riverbanks and a delta composed of tailings). Taylor et al. (1996) and Locher (1997) stated that the relative high density of sulfidic tailings and slags also constrained their distribution to the river bottom. The mass of tailings accumulated at each of these places was not a focus of this study, especially the river bottom, which could not be accessed. However, the high concentrations of pyrite reported (e.g. sites 7, 8, and 13; Table 2) and the medium to high-risk AMD potential of river samples by static tests, suggest that tailings are continuous sources of AMD in the Queen–King Rivers. Although Taylor et al. (1996) reported carbonates in tailings in the ranges of 0–5 wt%, in this study they were not identified in abundance in river sediments, indicating their possible dissolution over the years and likely insufficient abundance to buffer and attenuate the acid being produced. Comparing lab-based simulation of metal leaching, via NAG tests, to field-based water sampling suggests that the sediments do provide a source of dissolved metals to the river; however, this does not account for the full extent of metal loading observed in the Queen–King River system. A notable trend in water quality data is the decreased concentrations of Al, Cu, and Zn beginning around 2016 (Fig. 7I). Because no correlation between rainfall and dissolved metals were observed (Supplemental Fig. S-2), the deviation in the 20-year trend may be related to flooding of the lower levels of the Prince Lyell mine in 2016, which has decreased metals concentration in waters pumped from the mine (G. Cordery, personal communication, 2022). This suggests that prior to 2016, a large contribution of the metal concentrations observed over the duration of this study were derived from dewatering of underground mine waters that were in contact with mineralised zones (primarily chalcopyrite). This trend indicates that waste management efforts by CMT have been effective in reducing metal loading to the downstream environment. The reduced contribution from underground workings allows for the assessment of the contributions from legacy waste piles in the river. Whilst not yet stabilized, a diminishing trend in mass loading from 2016 (Fig. 7I) and

decrease in concentrations of trace metals, particularly at the high acid/high metal zone, indicate that legacy waste piles are an on-going, long-term source of contamination to the downstream environment. This is sourced by surface water flow through the sulfide-rich waste piles, which were generally placed around the perimeter of the open cut (Supplementary Fig. S-1; McQuade et al. 1995). These findings suggest that the tailings historically discharged at Haulage Creek, effluent pumped from underground mine workings, and seepage from exposed sulfidic waste rock piles constitute the primary sources of metal contamination in the Queen–King River system.

Baseline Water Quality

The West Queen River and King River above Queen (sites 1 and 10) are not affected by the tailings discharged into the Queen River. Overall, waters at both sites have circumneutral pH, and low conductivity and Eh values. These sites provide the best indicators of the natural baseline water quality of the area. However, with > 100 years of mining, logging, dam construction, and other industrial activities in the region, these cannot be considered pristine waters. The concentration of trace elements in the West Queen River sediments are above the ISQG-high (Fig. 3), suggesting the presence of mineralised rocks at or upstream of this site (Fig. 3; Corbett 2001b; Seymour et al. 2006) contributing to localised element enrichment in waters sourced in these catchments. Accordingly, dissolved metals such as Cu, Fe, and Zn (Fig. 7) are observed to be at concentrations above ANZECC guidelines. Leaching tests classify sediments from the West Queen River (site 1) in the acid zone (Fig. 8B) with $S = 0.17$ wt% (Supplementary Table S-4). These findings imply the presence of small quantities of sulfides in the local mineralisation (below XRD detection limits), that could be naturally weathering and generating acidity.

Long-Term Trends and Geochemical Drivers of AMD

Waters samples collected and analysed from the Queen–King River system can be divided into three sub-groups according to the Ficklin classification and water quality analysis: (1) low-metal, near-neutral waters; (2) metal-enriched, acid waters; (3) strongly metal-enriched, acid to high acid waters. The Eh is usually > 200 mV in the Queen–King River system. Group 1 is represented by baseline waters (sites 1 and 10), which have near neutral pH values with low concentrations of Al, Co, Cu, Fe, and Zn, and low Eh values (Fig. 7). Group 2 reflects sites 2, 3, 4, 11, 12, and 13, with near-neutral to acid pH values, and elevated dissolved metals, and Eh. Group 3 is considered

AMD waters, from sites 5 to 9, with highly acidic waters and elevated Eh, and contributes the greatest metal loading in the Queen–King River system.

In the Queen–King River system, pH and Eh influence the long-term stability of minerals and mobility of elements. This is particularly true at AMD-affected sites between Haulage Creek (site 5) and Lynchford (site 9), which have the lowest pH and highest Eh values. Such conditions enable dissolution of metals in the river (Fig. 9; Gäbler 1997). Overall, metal concentrations in water decrease with distance upstream (sites 2, 3, and 4) and downstream of Lynchford (22 km downstream of the source; sites 11, 12, and 13) where a decrease in Eh and an increase in pH are noted. This trend may be attributed to a combination of factors, including: (i) dilution from the large volume of uncontaminated tributary streams (baseline sites 1 and 10; Ghomshei and Allen 2000; Schmiermund and Drozd 1997), and: (ii) precipitation and sorption to the streambed driven by geochemical conditions (Huang et al. 2010). Despite this natural decrease, some dissolved metals are not sufficiently attenuated (Cu, Fe, and Zn) and remain above ANZECC guidelines (Fig. 7) until reaching the river terminus at Macquarie Harbour.

Table 4 compares the concentration ranges of Al, Co, Cu, Fe, and Zn dissolved in the Queen–King River system (2001–2021) with AMD/mine impacted waters in other regions around the globe. The metals selected were based on the main contaminants in the Queen–King River system, as reported in this study. Haulage Creek has higher concentrations of Al, Co, Cu, Fe, and Zn than many other contaminated waters shown, such as the Gyamaxung-chu,

Hudson, Pilcomayo, Azufre, Bor, and Bela rivers. That is also the case of the Lower Spring Creek site, which in the past drained mine effluents from the Iron Mountain mine, California, host of the most acidic waters known (Nordstrom et al. 2000), but currently represents a major successful case of AMD clean up in downstream catchments (U.S. Army Corps of Engineers 2018). In contrast, the Odiel and Tinto rivers, located in the Iberian Pyrite Belt, exhibit much higher dissolved metal concentrations than Haulage Creek.

Sediments from Haulage Creek and downstream (sites 5 and 6) have lower metal(lloid) contents than other acid drainage sites (sites 7, 8, and 9; Fig. 3, and Supplemental Table S-4). This increase of metal(lloid)s in the sediments from Haulage Creek to Lynchford might be attributed to: (i) leaching of metal(lloid)s from sediments at sites 5 and 6 driven by low pH and high Eh; (ii) leaching of metal(lloid)s in sediments driven by increased erosion at sites 5 and 6; (iii) metal(lloid)-rich mine effluents; and (iv) enrichments of sediments at sites 7, 8, and 9 caused by metal(lloid) precipitation. Figure 4 suggest metal(lloid)s hosted in Fe-bearing minerals at sites 7, 8, and 9, explained by sorption and/or coprecipitation of metal(lloid)s onto secondary minerals (Elghali et al. 2021).

Stream sediments and waters in the Queen and King Rivers have median trace metal(lloid) concentrations on the order of Cu > Zn > Co > Pb > As with Pb concentrations in the river (data not shown) below 0.1 mg·L⁻¹, and As content below 0.01 mg·L⁻¹ (Fig. 8C). In sediments, Pb and Zn behave coherently (Fig. 4, Table 1) and are likely from the same sources (e.g. sorbed onto Fe-oxyhydroxides; Swedlund 2004). The high correlation between As, Fe, and S suggest

Table 4 Concentration of dissolved metals in the Queen and King Rivers and other waters in the world

Location	Impact/distance	Al	Co	Cu	Fe	Zn	References
Queen and King rivers, Australia	Mine tailing, AMD	0.03–181.5	0.0001–3.0	0.004–70.9	0.1–1202.4	0.002–13.04	This study
Tinto river, Spain	Mine, AMD (0 km ^c)	4.6–740	0.03–5.3	1.3–115	0.3–1529	1.2–205	Olfás et al. (2020)
Odiel river, Spain	Mine, AMD (0 km ^c)	0.2–2580	0.06–47.8	0–440	0–5848	0–1437	Espana et al. (2005)
Gyamaxung-chu river, Tibet	Mine (< 1 km ^a)	0.01–11.34	0.001–0.07	0.1–16.0	0.02–0.38	0.0008–5.4	Huang et al. (2010)
Hudson river, USA	Mine, AMD (0.18 km ^a)	0.17–4.9	0.017–0.53	0.097–3.13	0.12–42.4	0.007–0.17	Gilchrist et al. (2009)
Pilcomayo river, Bolivia	Mine tailing, AMD (6 km ^b)	0.05–0.15	ND	0.01–0.08	0.02–6.0	0.3–8.8	Sun et al. (2020)
Bor and Bela rivers, Serbia	Mine tailings, AMD (5km ^a)	ND	ND	13.9–52.5	0.24–219	1.46–3.19	(Adamovic et al. 2021)
Azufre River, Chile	Mine tailings, AMD	70.1–156.9	ND	ND	32–85.5	6.3–12.6	(Guerra et al. 2016)
Lower Spring Creek, USA	Reabilitated AMD (2 km ^a)	ND	ND	0.05–0.15	0.3	0.09–0.8	(United States Army Corps of Engineers, 2018)

Concentrations are in mg·L⁻¹. Distances are from sampling locations to: (a) mineral processing site or mine entrance; (b) tailings discharge in the river; (c) AMD water discharge

ND no data

that pyrite is the main As source. In water, Cu and Zn have the greatest chemical mobility, whereas As and Pb display limited mobility, possibly due to their coprecipitation with Fe-oxyhydroxysulphate materials (Ashley et al. 2003; Lottermoser and Ashley 2006), or, in the case of As, its low concentrations (below ANZECC guidelines) in river sediments.

Data summarising the composition of AMD affected waters and NAG leachates (Fig. 8) indicates that sediments at Haulage Creek and downstream (sites 5 and 6) released less metals in NAG leachates than field waters. This finding corroborates that some of the bulk AMD originates from the underground mine and legacy waste pile rocks. The sediments containing the highest proportion of pyrite was detected in site 13 delta samples (Table 2), with liberated grains of this mineral noted (Fig. 5D). A high concentration of dissolved metals were also observed in the NAG leachates in contrast to low metal levels in the field water, indicating that while tailings are stored in the riverbanks and delta, they are compacted and not exposed to oxidizing conditions. The high proportion of liberated pyrite together with high metal dissolution under laboratory conditions suggests the potential exists for metal release and contamination of the river mouth and harbour under erosion and favourable geochemical conditions, and that the deltaic sediments provide a long-term source of AMD.

Pollution and Rehabilitation Options

This long-term study documents elevated quantities of metal loads and secondary precipitates in the Queen–King River system as consequence of historical mine waste discharge. The results are in accordance with previous post-mine closure research programs (Davies et al. 1996; Klessa et al. 1997; Koehnken 1997; McQuade et al. 1995; Miedecke 1996; Taylor et al. 1996), that evaluated the environmental effects of the AMD. Although a decreasing trend is observed from 2016, such findings highlight the serious and persistent contamination within this ecosystem nearly 30 years after riverine tailings disposal discontinued. This corroborates that without robust and effective remediation strategies, a long-term source of pollution remains in the river system. It also emphasizes the necessity to consider AMD potential when planning and operating mining projects. This level of pollution detrimentally affects aquatic life, whilst endemic plant species such as *Juncus pallidus* and some metal-tolerant ferns (Fig. 2, site 11) have thrived in this extreme environment.

Metal Recovery from AMD

Given the extent and scale of impacts, remediation and rehabilitation of the Queen–King River system would require costly and invasive strategies (Kefeni et al. 2017; Moodleya

et al. 2017), although, the extremely high concentrations of elements of economic interest found in the AMD could be of economic value (León et al. 2021). For example, the high concentration of metals, such as Cu, Co, and Zn (Fig. 7), indicate a potential source of valuable metals that might provide the opportunity to generate revenue while decreasing the environmental risk.

Experiments to examine recovery of metals from Mount Lyell AMD were considered in the past, with a pilot-scale plant involving solvent extraction (SX) and electrowinning (EW) being tested from 1991 to 1993 (Miedecke 1996). The financial analysis of SX/EW Cu recovery, based on 519 t per year of Cu production and a recovery efficiency of 80 wt% Cu gave an annual revenue of \$1.786 M, with annual operating costs of ≈ \$0.625 M and a net annual margin of \$1.161 M per annum (based on Cu price of US\$ 0.85 per lb at the time). This study showed that metal recovery from the Queen–King River could be financially viable, and able to potentially finance environmental improvements to the river quality. With the advent of new technologies since then, other alternatives are available.

Macingova and Luptakova (2012) reported the use of selective sequential precipitation (SSP) to produce high recovery of metals from AMD samples. The process has both chemical and biological treatment stages, with more than 99% of the Fe and Al selectively precipitated using a solution of NaOH, while 99% of Cu and Zn were recovered using biologically produced hydrogen sulfide. Assuming that all metal loads from mine dewatering would be available for recovery in the Queen–King Rivers and using the mass loads of 2021 (as calculated in kg.day⁻¹ for Austin St. Park (site 7), Fig. 7I) an annual revenue of \$1.229 M could be generated from Cu recovery, and a profit of \$0.123 M expected from Zn (Cu price of US \$9.89 per kg and Zn price of US \$3.40 per kg based on London Metal Exchange 2022). Tabak et al. (2003) also used SSP with both four- and six-stage metal sequential separation and biorecovery units that recovered 99.1% of the Co. Such metal recovery would correspond to US \$0.205 M of Co considering levels from Austin St. Park (Co price of \$56.55 per Kg based on London Metal Exchange 2022). In the study of Chen et al. (2014), ferrous ions were first oxidised by 0.15 mL/L 30% H₂O₂, and then a four-step fractional precipitation was applied with the selective addition of Ca(OH)₂ and Na₂S solutions. Results indicated recovery efficiencies of Fe, Cu, and Zn from AMD reaching 99.51%, 86.09%, and 87.87%, respectively. These results would represent an annual revenue of US \$1.069 M of Cu and US \$0.109 M of Zn for the metal loads determined at Austin St. Park.

Another potential source of valuable metals are the tailings stored in the Queen–King River system that nowadays are looked at as potentially exploitable and cost-saving raw materials (Lutandula and Maloba 2013). The north lobe

combined with Bank A have a spatial coverage of $\approx 0.59 \text{ km}^2$, the south lobe has 0.45 km^2 , and Bank D nearly 0.03 km^2 . Further attention should be placed on this material for detailed metal concentrations, mineralogy, and economic viability.

Limitations and Further Studies

The data collected for this study was acquired in an academic environment by UTAS students over two decades. The teaching staff and field assistants were meticulous in guiding students to accurately acquire samples and data. However, repeatability and reproducibility errors are inherent in this type of long-term study, especially due to the use of different measuring instruments and tools, multiple observers, conditions, and time constraints. Additionally, although it is important to estimate the returns that hypothetically could be generated to broaden the economic studies in the Queen–King Rivers, the mass loads obtained in this study do not represent average conditions over the year. Thus, calculations obtained here are sources of uncertainty because dissolved metals and flow rates can fluctuate through the year. Ideally, sampling should be implemented at least seasonally to observe fluctuations in dissolved metal concentrations. Furthermore, a hydrometallurgical program would provide a more reliable earnings forecast, particularly with regards to Cu and Co that reported higher returns in this study. The high flow rates and volume of water in the Queen–King River system would potentially pose challenges to future treatment. Nevertheless, any improvement in water quality through metal removal and/or acid neutralisation will be beneficial.

Conclusions

For over 100 years, the Mount Lyell mine operated in western Tasmania with limited management of waste and AMD. These by-products were discharged directly into Haulage Creek, draining into the Queen River, extending through the King River, with final outfall to Macquarie Harbour. The region displays an historical legacy of environmental impact. This extensive study evaluated the water quality in the Queen–King River system for 20 years to understand the impact of the discharge, level of contamination in the river, and the long-term sources of AMD. Our investigations demonstrate a change in the natural morphology of the river and its water quality over the years.

Waste piles, tailings, and mine effluents continue to contribute to the waste discharged in the Queen–King River system. From Haulage Creek to Lynchford, the Queen River is highly acid with dissolved metal concentrations above

ANZECC guidelines (e.g. Al, Co, Cu, Fe, and Zn). Mineralogical analysis at these sites revealed the precipitation of secondary minerals such as goethite and other poorly crystalline/amorphous Fe/S-bearing minerals, characteristic of AMD. Although diluted upstream of Haulage Creek and downstream of Lynchford, the river still exhibits impacts of mine discharge, evidenced by acidic waters enriched in dissolved metals (e.g. Cu, Fe, and Zn). Notably, from 2016 when Prince Lyell was flooded, mine effluents decreased in the Queen–King River system, and dissolved metals have declined in the river. However, contamination persists from waste rocks and tailings-rich sediments that have been deposited along the river bottom, riverbanks, and delta. Laboratory investigation showed high potential for long-term contamination of the river system due to the presence of metal-bearing and pyritic tailings within the sediment, especially at the delta. The West Queen and the King River above the Queen baseline sites indicate near-neutral pH with elevated dissolved metals (e.g. Cu, Fe, and Zn) from local mineralization. These are natural for this region and should act as remediation targets.

The present study highlights that nearly 30 years after historic waste disposal at the Queen–King system ceased, AMD still impacts the river. Unless remedial actions are taken, the Queen–King River system will continue to be severely affected for years to come, stressing the importance of debating AMD potential in mine projects. The prospect of metallurgical recovery (e.g. Cu, Co) is promising both environmentally and financially, and technologies such as SX/EW or SSP should be considered.

Supplementary Information The online version contains supplementary material available at <https://doi.org/10.1007/s10230-023-00943-5>.

Acknowledgements This research was funded by the Australian Research Council's Industrial Transformation Research Hub for Transforming the Mining Value Chain (project IH130200004). The authors acknowledge Elena Lounejeva (CODES, UTAS), Jay Thompson (CODES, UTAS), Nathan Fox (SMI, UQ), Thomas Rodemann (CSL), and Sandrin Feig (CSL, UTAS) for analytical assistance. We are grateful for ARC LIEF funding (LE0989539) for access to ICP-MS instrumentation, and we thank Geoff Cordery (Copper Mines Tasmania) and Sarah Gilmour (GHD) for SEM data. Thanks also to the Environmental Geology (KEA348) students who collected samples and observations over the past two decades (2001–2021).

Funding Open Access funding enabled and organized by CAUL and its Member Institutions.

Data availability The primary data associated with this manuscript have been included as Supplementary Material. Supporting data and further information on methods and materials are part of an on-going Ph.D. Thesis by the lead author and will be available online following its completion.

Open Access This article is licensed under a Creative Commons Attribution 4.0 International License, which permits use, sharing, adaptation, distribution and reproduction in any medium or format, as long

as you give appropriate credit to the original author(s) and the source, provide a link to the Creative Commons licence, and indicate if changes were made. The images or other third party material in this article are included in the article's Creative Commons licence, unless indicated otherwise in a credit line to the material. If material is not included in the article's Creative Commons licence and your intended use is not permitted by statutory regulation or exceeds the permitted use, you will need to obtain permission directly from the copyright holder. To view a copy of this licence, visit <http://creativecommons.org/licenses/by/4.0/>.

References

Adamovic D, Ishiyama D, Đorđevski S, Ogawa Y, Stevanovic Z, Kawaraya H, Sato H, Obradovic L, Marinkovic V, Petrovic J, Gardic V (2021) Estimation and comparison of the environmental impacts of acid mine drainage-bearing river water in the Bor and Majdanpek porphyry copper mining areas in eastern Serbia. *Resour Geol* 71:123–143. <https://doi.org/10.1111/rge.12254>

ANZECC (2000) Australian and New Zealand guidelines for fresh and marine water quality. Australian and New Zealand Environment and Conservation Council and Agriculture and Resource Management Council of Australia and New Zealand, Canberra

Ashley P, Lottermoser B, Chubb A (2003) Environmental geochemistry of the Mt Perry copper mines area, SE Queensland Australia. *Geochem-Explor Env A* 3(4):345–357. <https://doi.org/10.1144/1467-7873/03-014>

Augustinus P, Barton CE, Zawadzki A, Harle K (2010) Lithological and geochemical record of mining-induced changes in sediments from Macquarie Harbour, southwest Tasmania Australia. *Environ Earth Sci* 61(3):625–639. <https://doi.org/10.1007/s12665-009-0377-x>

Australian Broadcasting Corporation (2014) Mount Lyell copper mine: look back at key dates in the history of Australia's oldest mining field. <https://www.abc.net.au/news/2014-07-09/mount-lyell-timeline/5581684> Accessed 16 Apr 2022

Baird R, Bridgewater L (2017) Standard methods for the examination of water and wastewater. 23rd edit, American Public Health Assoc, vol 1, Washington DC

Bureau of Meteorology (2021) Climate statistics for Australian locations, Queenstown. http://www.bom.gov.au/climate/averages/tables/cw_097034_All.shtml Accessed 6 Jul 2022

Chen T, Yan B, Lei C, Xiao X (2014) Pollution control and metal resource recovery for acid mine drainage. *Hydrometallurgy* 147–148:112–119. <https://doi.org/10.1016/j.hydromet.2014.04.024>

Corbett K (1976) Notes on the volcanic stratigraphy and Cambro-Ordo-vician relationships in the Mt Jukes area. Unpublished Report. Dept of Mines, Tasmania, p 49

Corbett KD (2001a) The geology of the Mount Lyell mines area, Tasmania: a re-interpretation based on studies at Lyell Comstock, North Lyell and the Iron Blow area. Research MS thesis, Univ of Tasmania

Corbett KD (2001b) New mapping and interpretations of the Mount Lyell mining district, Tasmania: a large hybrid Cu–Au system with an exhalative Pb–Zn top. *Econ Geol* 96(5):1089–1122. [\(1554-0774\)](https://doi.org/10.2113/gsecongeo.96.5.1089)

Davies P, Mitchell N, Barmuta L (1996) The impact of historical mining operations at Mount Lyell on the water quality and biological health of the King and Queen River catchments, western Tasmania. Mount Lyell Remediation R&D Program, Supervising Scientist Report, vol 118

Durocher J, Schindler M (2011) Iron-hydroxide, iron-sulfate and hydrous-silica coatings in acid-mine tailings facilities: a comparative study of their trace-element composition. *Appl Geochem* 26:1337–1352. <https://doi.org/10.1016/j.apgeochem.2011.05.007>

EGI (1991) Investigation of the geochemical of the Delta on the King River entering Macquarie Harbour. Report no. 3 prepared by Environmental Geochemistry International for the Mt. Lyell Mining and Railway Company Ltd

EGI (1993) Modelling of water quality in the Queen and King rivers below the Mount Lyell Mine. Consultant report no. 5, Report prepared by Environmental Geochemistry International for the Mt. Lyell Mining and Railway Company Ltd

Elghali A, Benzaazoua M, Bouzahzah H, Abdelmoula M, Dynes JJ, Jamieson HE (2021) Role of secondary minerals in the acid generating potential of weathered mine tailings: crystal-chemistry characterization and closed mine site management involvement. *Sci Total Environ* 784:147105. <https://doi.org/10.1016/j.scitotenv.2021.147105>

EPA Tasmania (2013) Mt Lyell acid drainage remediation. <https://epa.tas.gov.au/epa/water/remediation-programs/mt-lyell-acid-drainage-remediation> Accessed 21 Apr 2021

España J (2007) The behavior of iron and aluminum in acid mine drainage: speciation, mineralogy, and environmental significance. In: Letcher TM (ed) Ch 7, thermodynamics, solubility and environmental issues. Elsevier, pp 137–150

Espana JS, Pamo EL, Santofimia E, Aduvire O, Reyes J, Baretino D (2005) Acid mine drainage in the Iberian Pyrite Belt (Odiel river watershed, Huelva, SW Spain): geochemistry, mineralogy and environmental implications. *Appl Geochem* 20(7):1320–1356. <https://doi.org/10.1016/j.apgeochem.2005.01.011>

Gäbler H-E (1997) Mobility of heavy metals as a function of pH of samples from an overbank sediment profile contaminated by mining activities. *J Geochem Explor* 58(2–3):185–194. [https://doi.org/10.1016/S0375-6742\(96\)00061-1](https://doi.org/10.1016/S0375-6742(96)00061-1)

Ghomshie M, Allen D (2000) Hydrochemical and stable isotope assessment of tailings pond leakage, Nickel Plate Mine, British Columbia. *Environ Geol* 39:937–944. <https://doi.org/10.1007/s002549900064>

Gilchrist S, Gates A, Szabo Z, Lamothe PJ (2009) Impact of AMD on water quality in critical watershed in the Hudson River drainage basin: Phillips Mine, Hudson Highlands New York. *Environ Geol* 57(2):397–409. <https://doi.org/10.1007/s00254-008-1310-4>

Guerra P, Simonson K, González C, Gironás J, Escuariaza C, Pizarro G, Bonilla C, Pasten P (2016) Daily Freeze–thaw cycles affect the transport of metals in streams affected by acid drainage. *Water* 8:74. <https://doi.org/10.3390/w8030074>

Guo H, Barnard A (2013) Naturally occurring iron oxide nanoparticles: morphology, surface chemistry and environmental stability. *J Mater Chem A* 1:27–42. <https://doi.org/10.1039/C2TA00523A>

Huang X, Sillanpää M, Gjessing ET, Peräniemi S, Vogt RD (2010) Environmental impact of mining activities on the surface water quality in Tibet: Gyama valley. *Sci Total Environ* 408(19):4177–4184. <https://doi.org/10.1016/j.scitotenv.2010.05.015>

Huston DL, Kamprad J (2001) Zonation of alteration facies at western Tharsis: implications for the genesis of Cu–Au deposits, Mount Lyell field Western Tasmania. *Econ Geol* 96(5):1123–1132. [\(1554-0774\)](https://doi.org/10.2113/gsecongeo.96.5.1123)

Kefeni KK, Msagati TAM, Mamba BB (2017) Acid mine drainage: prevention, treatment options, and resource recovery: a review. *J Clean Prod* 151:475–493. <https://doi.org/10.1016/j.jclepro.2017.03.082>

Klessa D, Koehnken L, Johnston J (1997) Estimation of water quality over time within the Queen and King Rivers. Mount Lyell Remediation Research and Demonstration Program. Supervising Scientist Report, vol 121

Koehnken L (1997) Mount Lyell remediation: final report. Mount Lyell Remediation Research and Demonstration Program. Supervising scientist report, vol 126,

León R, Macías F, Cánovas RC, Pérez-López R, Ayora C, Nieto JM, Olías M (2021) Mine waters as a secondary source of rare earth

elements worldwide: the case of the Iberian Pyrite Belt. *J Geochem Explor* 224:106742. <https://doi.org/10.1016/j.gexplo.2021.106742>

Locher H (1997) Sediment transport in the King River, Tasmania. Mount Lyell remediation research and demonstration program. Supervising Scientist Report. 120:124

London Metal Exchange (2022) The London metal exchange, the world centre for industrial metals trading. <https://www.lme.com/> Accessed 27 Oct 2022

Lottermoser BG, Ashley PM (2006) Mobility and retention of trace elements in hardpan-cemented cassiterite tailings, north Queensland, Australia. *Environ Geol* 50(6):835–846. <https://doi.org/10.1007/s00254-006-0255-8>

Lutandula MS, Maloba B (2013) Recovery of cobalt and copper through reprocessing of tailings from flotation of oxidised ores. *J Environ Chem Eng* 1(4):1085–1090. <https://doi.org/10.1016/j.jece.2013.08.025>

Macingova E, Luptakova A (2012) Recovery of metals from acid mine drainage. *J Chem Eng Trans* 28:109–114. <https://doi.org/10.3303/CET1228019>

McQuade CV, Johnston JF, Innes SM (1995) Mount Lyell Remediation: review of historical literature and data on the sources and quality of effluent from the Mount Lyell lease site, Supervising Scientist Report No. 0642243034

Miedecke J (1996) Remediation options to reduce acid drainage from historical mining operations at Mount Lyell, Western Tasmania. Mount Lyell Remediation Research and Demonstration Program. Supervising Scientist Report, vol 108

Moodleya I, Sheridana CM, Kappelmeyer U, Akcild A (2017) Environmentally sustainable acid mine drainage remediation: research developments with a focus on waste/by-products. *Miner Eng*. <https://doi.org/10.1016/j.mineng.2017.08.008>

Mt Lyell (1990) Physical impact of tailings discharge on Queen and King River systems. Report commissioned for the Mt Lyell Mining and Railway Company

Nordstrom D, Alpers C, Ptacek C, Blowes D (2000) Negative pH and extremely acidic mine waters from iron mountain, California. *Environ Sci Technol* 34:254–258. <https://doi.org/10.1021/es990646v>

Olías M, Cánovas CR, Macías F, Basallote MD, Nieto JM (2020) The evolution of pollutant concentrations in a river severely affected by acid mine drainage: Río Tinto (SW Spain). *Minerals* 10(7):598. <https://doi.org/10.3390/min10070598>

Olive LJ, Reiger WA (1986) Low Australia sediment yields—a question of inefficient delivery. In: Hadley RF (ed), *Drainage basin sediment delivery*, Proc, International Assoc of Hydrological Sciences Symp, IAHS Publ no. 159, pp 355–364

Plumlee GS, Logsdon MJ, Filipek LH (1999) The environmental geochemistry of mineral deposits; Part A: processes, techniques, and health issues; Part B: case studies and research topics. *Rev Econ Geol*. <https://doi.org/10.5382/Rev.06>

Price WA (1997) Guidelines and recommended methods for the prediction of metal leaching and acid rock drainage at minesites in British Columbia; draft. Energy and Minerals Div, Ministry of Employment and Investment

Qian G, Li Y (2019) Acid and metalliferous drainage—a global environmental issue. *JOMME* 1(1):1–4. <https://doi.org/10.32474/JOMME.2019.01.000101>

Schmiermund R, Drozd M (1997) Acid mine drainage and other mining-influenced waters (MIW). *Mining Environmental Handbook: Effects of Mining on the Environment and American Environmental Controls on Mining*, World Scientific, pp 599–617

Seymour D, Green G, Calver C (2006) The geology and mineral deposits of Tasmania: a summary. vol 72, 2nd edn, Tasmanian Dept of Infrastructure, Energy and Resources

Sheoran AS, Sheoran V (2006) Heavy metal removal mechanism of acid mine drainage in wetlands: a critical review. *Miner Eng* 19(2):105–116. <https://doi.org/10.1016/j.mineng.2005.08.006>

Smart R, Skinner W, Levay G, Gerson A, Thomas J, Sobieraj H, Schumann R, Weisener C, Weber P, Miller S (2002) ARD test handbook: project P387A, prediction and kinetic control of acid mine drainage. AMIRA, International Ltd, Ian Wark Research Institute, Melbourne, Australia

Solomon M, Vokes F, Walshe J (1987) Chemical remobilization of volcanic-hosted sulphide deposits at Rosebery and Mt. Lyell, Tasmania. *Ore Geol Rev* 2(1–3):173–190. [https://doi.org/10.1016/0169-1368\(87\)90027-8](https://doi.org/10.1016/0169-1368(87)90027-8)

Sun J, Strosnider WHJ, Nairn RW, LaBar JA (2020) Water quality impacts of in-stream mine tailings on a headwater tributary of the Rio Pilcomayo Potosí Bolivia. *J Appl Geochem* 113:104464. <https://doi.org/10.1016/j.apgeochem.2019.104464>

Swedlund PJ (2004) Modelling Cu, Zn, Cd and Pb adsorption by iron oxyhydroxides in SO_4 -rich systems simulating acid mine drainage. PhD thesis, Univ of Auckland

Tabak HH, Scharp R, Burckle J, Kawahara FK, Govind R (2003) Advances in biotreatment of acid mine drainage and biorecovery of metals: 1. Metal precipitation for recovery and recycle. *Biodegradation* 14(6):423–436. <https://doi.org/10.1023/A:1027332902740>

Taylor JR, Weaver TR, McPhail DB, Murphy NC (1996) Characterization and impact assessment of mine tailings in the King River system and delta, western Tasmania. Mount Lyell Remediation Research and Demonstration Program, Supervising Scientist Report 105, vol 105

Townsend AT (1999) The determination of arsenic and selenium in standard reference materials using sector field ICP-MS in high resolution mode. *Fresenius J Anal Chem* 364(6):521–526. <https://doi.org/10.1007/s002160051379>

Townsend AT (2000) The accurate determination of the first row transition metals in water, urine, plant, tissue and rock samples by sector field ICP-MS. *J Anal at Spectrom* 15(4):307–314

US Army Corps of Engineers (2018) 6th 5-year review report for Iron Mountain Mine superfund site Shasta county, California report. US Environmental Protection Agency

Walshe J, Solomon M (1981) An investigation into the environment of formation of the volcanic-hosted Mt. Lyell copper deposits using geology, mineralogy, stable isotopes, and a six-component chlorite solid solution model. *Econ Geol* 76(2):246–284

Weber P, Hughes J, Conner L, Lindsay P, Smart C (2006) Short-term acid rock drainage characteristics determined by paste pH and kinetic NAG testing: cypress prospect, New Zealand. *JASMR* 2006:2289–2310. <https://doi.org/10.21000/JASMR06022289>

Williamson M, Kirby C, Rimstidt J (2006) Iron dynamics in acid mine drainage. *JASMR* 2006:2411–2423. <https://doi.org/10.21000/JASMR06022411>